Preprints of the 19th World Congress
The International Federation of Automatic Control
Cape Town, South Africa. August 24-29, 2014

Modeling and Control of Rotor-Flying Multi-Joint Manipulator ⋆

Bin Yang [*,**] **Yuqing He** [**] **Jianda Han** [**] **Guangjun Liu** [***]

[*] *University of Chinese Academy of Sciences, Beijing 100049, China; (e-mail:yangbin@sia.cn)*
[**] *State Key Laboratory of Robotics ,Shenyang Institute of Automation Chinese Academy of Sciences, Shenyang 110016, China*
[***] *Ryerson University Toronto, Ontario, Canada M5B 2K3*

Abstract: Equipping manipulators on a mobile robot to actively influence its surroundings has been extensively used in many ground robots,underwater robots and space robots systems. However, it is difficult to make such re-design in a Rotor Flying Robot (RFR). This is mainly because 1)the equipped manipulator will bring heavy coupling between it and the RFR system, which makes the whole system model highly complicated and makes the central controller design impossible. 2)the movement of the manipulator will introduce a great deal time-varying disturbance to the RFR system, which makes distributed control design also challenging. Thus, in this paper, utilizing the Euler-Lagrange equation, the highly accurate dynamics model of a combined system, called Rotor-Flying Multi-Joint Manipulator (RF-MJM), is constructed and its complexity is analyzed and presented. Then, a linearized full-state feedback Linear Quadratic Regulator (LQR)controller is designed for the aircraft to hover near a trim point. Finally, simulations using MATLAB are conducted and the results are analyzed to show the basic control performance of the LQR controller.

Keywords: manipulator,Rotor Flying Robot,trim point, Linearization, Euler-Lagrange equation .

1. INTRODUCTION

Rotor Flying Robot (RFR), a special kind of unmanned aerial vehicle (UAV), has been researched for several decades and achieved great development. To date, RFRs have been applied in many kinds of fields, such as search , rescue and surveillance, etc. (Valavanis (2007), Birk et al. (2011), Bolkcom (2004), Cai et al. (2010), Puri (2005)).

However, most of existing RFR systems cannot be used to implement the so called active task, i.e., manipulate objects of interest. These abilities are sometimes required, e.g., for the precise delivery of escape tools in a fire.

Recently, this problem has attained much attention from researchers. In (Mellinger et al. (2013),Bernard and Kondak (2009),Pounds et al. (2011)) different kinds of grippers are equipped the RFR system to make the latter be able to manipulate the extend objects. These above researches show the basic feasibility of the new idea.

The aforementioned achievements show that most the existing rotor flying manipulator systems equip only claw with small mass compared to the RFR itself, so that the influence of the claw on RFR is ignorable and the flying performance can be ensured. Unfortunately, this kind of infrastructure has several obvious disadvantages: 1)The manipulator space is very limited because the manipulator can only be moved through movability of the RFR system. This results in another disadvantage 2) the control performance is difficult to be ensured and precise manipulation is impossible. This is mainly because the precise control of the RFR system is impossible due to the complicated and uncertain aerodynamics, especially when RFR is close to the objects.

Thus , in this paper, a new system is proposed to overcome the above disadvantages. The system is depicted in Fig.1, and is called Rotor -Flying Multi-Joint Manipulator(RF-MJM). This system is composed of an RFR system and a multi-joint manipulator. Its main features are the multiple joints of the manipulator which can be used to regulate the position and attitude of the end-gripper, this is useful to compensate the imprecise control of the RFR system. However, some problems are also introduced accompanied by the above advantage. For example, the structure of the whole RF-MJM system is of great complexity, which will result in high nonlinearities and thus introduce more difficulties into the controller design.

To deal with this problem, the dynamics model of the RF-MJM system is constructed and analyzed in this paper to verify some basic performances. Also, a linear-quadratic regulator (LQR) controller is designed to test the basic closed loop performance.

Fig. 1. the RF-MJM system with 3-DOF arm

The paper is organized as follows .Section2 derives the kinematics and dynamics model of RF-MJM. In Section3, we lin-

⋆ This work was supported by the National Natural Science Foundation of China (61305120).

earize the dynamic model near a trim point and design a full state feedback LQR controller. In Section4, two simulations are conducted to test the control performance of the RF-MJM system .Finally ,conclusions are drawn in Section5.

2. SYSTEM MODELING

2.1 System Description

Considering a RF-MJM system as shown in Fig.1. It is constituted of two subsystems: RFR and a n-DOF link rigid robotic manipulator. Each link of the manipulator is torque-driven by a DC servo motor. To model the RF-MJM system, we have the following assumptions:(a) the whole RFR is a rigid body. (b) Every link between two joints is rigid. Under these assumptions, the RF-MJM system can be modeled as a multi-link system illustrated in Fig.2 and its dynamical model can be derived using the Euler-Lagrange formulation. Some symbols

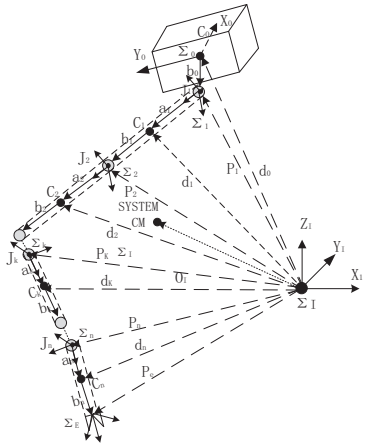

Fig. 2. a general model of RF-MJM having a n DOF(degrees of freedom) manipulator

and variables are defined as follows:
$\sum_I$: Earth-fixed inertial frame
$\sum_0$: Body-fixed reference frame
$\sum_E$: End-effector frame
$\sum_k$: Frame of the k-th joint of manipulator, k=1,...,n
C_k : Position vector of the center of mass (COM) of link k, k=0,1,...,n
J_k : Joint between the link k-1 and k of the manipulator, k=1,...,n
a_k : Vector from J_k to C_k ,k=1,2,...,n-1
b_0 : Vector from centroid of rotor flying robot to the first joint
b_k : Link vector from C_k to J_{k+1},k=1,2,...,n-1
m_k : Mass of link k(k=0,1,...,n).
I_k : Inertia tensor of link k with respect to its mass center, k=0,1,...,n
$\Theta = [\theta_1, \theta_2, ..., \theta_n]^T \in R^{n\times 1}$joint angular position vector
d_0 : Position vector of the RFR
d_i : Position vector of the COM of link i,i=1,2,...,n
d_g : Position vector of the COM of the RF-MJM
x_b : Pose vector of the RFR
x_e : Pose vector of the end-effector
d_e : Position vector of the end-effector
p_k : Position vector of J_k
v_0 : Linear velocity of the RFR
v_k : Linear velocity of the COM of the link k
v_e : Linear velocity of the end-effector
ω_0 : Angular velocity of the RFR in the inertial frame
ω_k : Angular velocity of the link k in the inertial frame
ω_e : Angular velocity of the end-effector
ϖ : The total mass of rotor flying robot and manipulator
k_k : Unit vector of z axis of link i in the i-th coordinate system
R_i^I : Coordinate transformation matrix from the frame of link i to Earth-fixed inertial frame
$C_{i,i}$: the position vector from joint i to the COM of link i in the i-th joint coordinate system.
$*$ The following vectors are in the inertial frame unless specially indicated.

2.2 kinematic equation of RF-MJM

The position vector of each link can be denoted as

$$d_i = d_0 + b_0 + \sum_{k=1}^{i-1}(a_k + b_k) + a_i \tag{1}$$

differentiate it with respect to time,we have

$$v_i = \dot{d}_i = v_0 + \omega_0 \times (d_i - d_0) + \sum_{k=1}^{i}\{k_k \times (d_i - p_k)\}\dot{\theta}_k \tag{2}$$

the angular velocity of each link can be described as

$$\omega_i = \omega_0 + \sum_{k=1}^{i} k_k \dot{\theta}_k \tag{3}$$

combining (2)and (3),we have

$$[\, v_i \;\; \omega_i \,]^T = \bar{J}_{bi}[\, v_0 \;\; \omega_0 \,]^T + \bar{J}_{mi}\dot{\Theta} \tag{4}$$

where $\bar{J}_{b_i}$ is Jacobian Matrix of the rotor flying robot

$$\bar{J}_{b_i} = \begin{pmatrix} E & -\tilde{d}_{0i} \\ 0 & E \end{pmatrix} = \begin{bmatrix} \bar{J}_{bv_i} \\ \bar{J}_{b\omega_i} \end{bmatrix}, \;\; d_{0i} = d_i - d_0 \tag{5}$$

$\bar{J}_{bv_i}$, $\bar{J}_{b\omega_i}$ in (5) are a block matrix of $\bar{J}_{b_i}$, E is the unity matrix, d_{0i} is as follows,

$$d_{0i} = [\, d_x \;\; d_y \;\; d_z \,]^T$$

,then $\tilde{d}_{0i}$ is the 3 x 3 skew-symmetric matrix. J_{m_i} is defined as

$$\bar{J}_{m_i} = \begin{bmatrix} k_1 \times (p_{i+1} - p_1) & \cdots & k_n \times (p_{i+1} - p_n) \\ k_1 & \cdots & k_n \end{bmatrix} = \begin{bmatrix} \bar{J}_{mv_i} \\ \bar{J}_{m\omega_i} \end{bmatrix} \tag{6}$$

k_i is the unit vector of axis Z_i in the joint frame. v_0 is defined as,

$$v_0 = \begin{bmatrix} \mathrm{c}\theta\mathrm{c}\varphi & \mathrm{s}\phi s\theta\mathrm{c}\varphi - c\phi s\varphi & \mathrm{c}\phi\mathrm{s}\theta\mathrm{c}\varphi + \mathrm{s}\phi\mathrm{s}\varphi \\ \mathrm{c}\theta\mathrm{s}\varphi & \mathrm{c}\phi\mathrm{c}\varphi + \mathrm{s}\theta\mathrm{s}\phi\mathrm{s}\varphi & \mathrm{c}\phi\mathrm{s}\theta\mathrm{s}\varphi - \mathrm{s}\phi\mathrm{c}\varphi \\ -\mathrm{s}\theta & s\phi c\theta & \mathrm{c}\phi c\theta \end{bmatrix} \begin{bmatrix} u \\ v \\ w \end{bmatrix} \tag{7}$$

where *c means cos*, *s means sin*. ϕ, θ, ψ represent the attitude of the RFR (roll, pitch, yaw), respectively. u, v, w are the components of the linear velocity along the axes of the body-fixed reference frame, v_0 is the linear velocity of the RFR.The relation between the angular velocity in Earth Frame and Body Frame is as follows.

$$\omega_0 = \begin{bmatrix} 1 & \sin\phi\tan\theta & \cos\phi\tan\theta \\ 0 & \cos\phi & -\sin\phi \\ 0 & \sin\phi\sec\theta & \cos\phi\sec\theta \end{bmatrix} \begin{bmatrix} p \\ q \\ r \end{bmatrix} \tag{8}$$

where p, q, r are the components of the angular velocity along the axes of the body-fixed reference frame.

2.3 Dynamic Model

A. Kinetic Energy of RF-MJM
Define a generalized velocity of the whole system as $\dot{q} = [v_0, \omega_0, \dot{\Theta}]$(Yoshida and Umetani (1993)). So the kinetic energy of the system can be denoted as

$$E_K = \frac{1}{2}\sum_{i=0}^{n}(\omega_i^T I_i \omega_i + m_i v_i^T v_i) \tag{9}$$

where the first term is kinetic energy due to angular velocity, the second term is kinetic energy due to linear velocity, then substituting (2) and (3) into (9),we have

$$E_k = \frac{1}{2}\begin{bmatrix} v_0 \\ \omega_0 \\ \dot{\Theta} \end{bmatrix}^T \begin{bmatrix} \varpi E & \varpi \tilde{d}_{0g}^T & J_{T\omega} \\ \varpi \tilde{d}_{0g} & H_\omega & H_{\omega\phi} \\ J_{T\omega}^T & H_{\omega\phi}^T & H_m \end{bmatrix} \begin{bmatrix} v_0 \\ \omega_0 \\ \dot{\Theta} \end{bmatrix} \quad (10)$$

where H is the inertia matrix of RF-MJM.

$$H_m = \sum_{i=1}^{n} (J_{Ri}^T I_i J_{Ri} + m_i J_{Ti}^T J_{Ti}) \in R^{n\times n}$$
$$J_{Ri} = [k_1, k_2, \cdots, k_i, 0, \cdots, 0] \in R^{3\times n}$$
$$J_{Ti} = [k_1 \times (p_2 - p_1), \cdots, k_i \times (d_i - p_i), 0, \cdots, 0] \in R^{3\times n}$$
$$J_{T\omega} = \sum_{i=1}^{n} (m_i J_{Ti}) \in R^{3\times n}$$
$$H_\omega = \sum_{i=1}^{n} (I_i + m_i \tilde{d}_{0i}^T \tilde{d}_{0i}) + I_0 \in R^{3\times n}$$
$$H_{\omega\phi} = \sum_{i=1}^{n} (I_i J_{Ri} + m_i \tilde{d}_{0i} J_{Ti}) \in R^{3\times n}$$
$$d_{0g} = d_g - d_0, d_g = \sum_{i=0}^{n} m_i d_i / \sum_{i=0}^{n} m_i$$

where I_0 is the inertia tensor of the rotor flying robot.

B. Potential Energy of RF-MJM

From (1),position vector of centroid of rigid body systems is rewritten as follows,

$$d_i = d_0 + \sum_{j=1}^{i} ({}^I A_{j-1} * C_{j-1,j} - {}^I A_j * C_{j,j}) \quad (11)$$

thus, the potential energy of the system due to gravity is as follows,

$$E_p = -\sum_{i=0}^{n} m_i g^T \left[d_0 + \sum_{j=1}^{i} ({}^I A_{j-1} * C_{j-1,j} - {}^I A_j * C_{j,j}) \right] \quad (12)$$

$$C_{i,i} = \begin{cases} [\,0\ 0\ 0\,]^T, & i = 0 \\ [\,-l_i\ 0\ 0\,]^T, & i \neq 0 \end{cases} \quad (13)$$

$$C_{i-1,i} = \begin{cases} [\,0\ 0\ -L_0\,]^T, & i = 1 \\ [\,L_i\ 0\ 0\,]^T, & i > 1 \end{cases} \quad (14)$$

where ${}^I A_0$ represents coordinate transformation matrix from the body-fixed reference frame to Earth-fixed inertial frame and ${}^I A_i$ denotes i-th joint coordinate to Earth-fixed inertial frame . l_i is the length from joint i to the COM of link i in the i-th joint coordinate system. L_i is the length from the COM of link i to the joint i+1 in the i-th joint coordinate system.

C. Dynamic Equation of RF-MJM

The Euler-Lagrangian equation of RF-MJM is

$$L = E_K - E_p \quad (15)$$

thus,the dynamic model of the system can be obtained by

$$\frac{d}{dt}\left(\frac{\partial L}{\partial \dot{q}}\right) - \frac{\partial L}{\partial q} = \tau \quad (16)$$

where $q = [X, \Phi, \Theta], \dot{q} = [v_0, \omega_0, \dot{\Theta}]$, X, Φ are position and RPY(roll,pitch,yaw) angle of rotor flying robot, Θ are angles of joints of the manipulator, τ is the external force and moment vectors. (16) can also be expressed as the following,

$$\begin{bmatrix} H_b & H_{bm} \\ H_{bm}^T & H_m \end{bmatrix} \begin{bmatrix} \ddot{x}_b \\ \ddot{\Theta} \end{bmatrix} + \begin{bmatrix} C_b \\ C_m \end{bmatrix} + \begin{bmatrix} G_b \\ G_m \end{bmatrix} = \begin{bmatrix} F_P \\ \tau_m \end{bmatrix} \quad (17)$$

where $\ddot{x}_b = \begin{bmatrix} \dot{v}_0^T & \dot{\omega}_0^T \end{bmatrix}^T$, $\dot{v}_0$, $\dot{\omega}_0$ are the linear acceleration and angular acceleration of the rotor flying robot,respectively; $\ddot{\Theta}$ is the joint angular acceleration of the manipulator; C_b, C_m are Coriolis and centrifugal force and manipulator, respectively; G_b, G_m are potential energy items of rotor flying robot and manipulator, respectively. τ_m is the torques of each servomotor of the manipulator.

$$F_P = \begin{bmatrix} F_B \\ M_B \end{bmatrix}, F_B = \begin{bmatrix} X \\ Y \\ Z \end{bmatrix}, M_B = \begin{bmatrix} L \\ M \\ N \end{bmatrix}, C_b = \begin{bmatrix} C_{bv} \\ C_{b\omega} \end{bmatrix}$$
$$G_b = \begin{bmatrix} G_{bv} \\ G_{b\omega} \end{bmatrix}, H_b = \begin{bmatrix} H_{b_{11}} & H_{b_{12}} \\ H_{b_{21}} & H_{b_{22}} \end{bmatrix}_{2\times 2}, H_{bm} = \begin{bmatrix} H_{bmv} \\ H_{bm\omega} \end{bmatrix}_{2\times 1}$$

where $H_{b_{11}} = \varpi E, H_{b_{12}} = \frac{1}{2}\varpi \tilde{d}_{og} + \frac{1}{2}\varpi \tilde{d}_{og}^T$

$$H_{b_{21}} = \tfrac{1}{2}\varpi \tilde{d}_{og}^T + \tfrac{1}{2}\varpi \tilde{d}_{og}\ ,\ H_{b_{22}} = H_\omega$$

$$H_{b_{mv}} = \tfrac{1}{2} J^T{}_{T\omega} + \tfrac{1}{2} J_{T\omega}, H_{bm\omega} = \tfrac{1}{2} H^T{}_{\omega\phi} + \tfrac{1}{2} H_{\omega\phi}$$

$$C_{bv} = \tfrac{1}{2}\omega_0{}^T \dot{\varpi} d_{og} + \tfrac{1}{2}\varpi \dot{d}^T{}_{og}\omega_0 + \tfrac{1}{2}\dot{\Theta}^T J_{T\omega}^T + \tfrac{1}{2} J_{T\omega}\dot{\Theta}$$

$$C_{b\omega} = \frac{1}{2}\dot{\varpi} d_{og} v_0 + \frac{1}{2} v_0{}^T \dot{\varpi} \dot{d}^T{}_{og} + \dot{H}_\omega \omega_0 + \frac{1}{2}\dot{\Theta}^T \dot{H}_{\omega\phi}^T + \frac{1}{2}\dot{H}_{\omega\phi}\dot{\Theta}$$

$$C_m = \tfrac{1}{2}\dot{J}_{T\omega}^T v_0 + \tfrac{1}{2} v_0^T \dot{J}_{T\omega} + \tfrac{1}{2}\dot{H}_{\omega\phi}^T \omega_0 + \tfrac{1}{2}\omega_0^T \dot{H}_{\omega\phi} + \dot{H}_m \dot{\Theta}$$

$$G_{bv} = \tfrac{\partial E_p}{\partial X}\ ,\ G_{b\omega} = \tfrac{\partial E_p}{\partial \Phi}\ ,\ G_m = \tfrac{\partial E_p}{\partial \Theta}$$

For an RFR,it is well known that $C_{bv} = 0$,$C_{bw} = \frac{1}{2} C_{\omega 4}\omega_0$ (Shim (2000),Bramwell et al. (2001)).Thus ,compared to the RFR,the proposed RF-MJM system will have to face the following difficulties.

1)Due to the appearance of some new terms, such as C_{bv}, the system clearly presents a more complex structure, which makes some existing control algorithm that is fit for RFR system cannot be used directly. For example in reference(He and Han (2010)), a RFR is proved to be approximate feedback linearization since the coupling between rolling(pitching)moments and lateral(longitudinal)acceleration is relatively small. However, for the RF-MJM system, the similar term is enlarged greatly because of the coupling between the RFR and the manipulator. Thus, even approximate feedback linearization is not possible.

2)Since the mass and size of the manipulator cannot be ignored with respect to the RFR system, the motion of the manipulator will inevitably influence the motion of the RFR system. This can be seen clearly in simulation result in the following sections,which shows that the whole system presents heavy nonlinearities and the controller design is challenging.

D. Extended Model

When the manipulator contact with external objects , the dynamics model becomes

$$\begin{bmatrix} H_b & H_{bm} \\ H_{bm}^T & H_m \end{bmatrix} \begin{bmatrix} \ddot{x}_b \\ \ddot{\Theta} \end{bmatrix} + \begin{bmatrix} C_b \\ C_m \end{bmatrix} + \begin{bmatrix} G_b \\ G_m \end{bmatrix} = \begin{bmatrix} F_P \\ \tau_m \end{bmatrix} + \begin{bmatrix} J_b^T \\ J_m^T \end{bmatrix} F_e \quad (18)$$

where F_e is the force and torque exerted on the end of the manipulator, J_b is the Jacobian matrix defined as,

$$J_b = \begin{pmatrix} E & -\tilde{p}_{0i} \\ 0 & E \end{pmatrix} = \begin{bmatrix} J_{bv} \\ J_{b\omega} \end{bmatrix}, p_{0i} = p_i - d_0$$

where J_{bv} and $J_{b\omega}$ are block matrix of J_b ,representing the linear and angular velocities ,respectively. J_m is defined as

$$J_m = \begin{bmatrix} k_1 \times (p_e - p_1) & \cdots & k_n \times (p_e - p_n) \\ k_1 & \cdots & k_n \end{bmatrix} = \begin{bmatrix} J_{mv} \\ J_{m\omega} \end{bmatrix}$$

furthermore , if considering the aerodynamics of rotor flying robot and ignoring the effect of aerodynamics on manipulator, we can get the general force and moment of the RFR and express them by the following mathematical equations(He and Han (2010)).

$$X = -T_M \sin a_{1s}, Y = T_M \sin b_{1s}$$
$$Z = -T_M \cos a_{1s} \cos b_{1s}$$
$$L = S_{L1} b_{1s} + S_{L2} Q_M$$
$$M = S_{M1} a_{1s} + S_{M2} T_M + S_{M3} Q_T$$
$$N = S_{N1} Q_M + S_{N2} T_T$$

where T_M and T_T are the forces exerted on the main rotor and tail rotor, a_{1s} and b_{1s} stand for the longitudinal and lateral flapping angle of main rotor, respectively; the forces T_M and T_T and the moments Q_M and Q_T can be calculated as(Shim (2000)). Thus ,we have

$$F_P = [\, X \;\; Y \;\; Z \;\; L \;\; M \;\; N \,]^T$$

putting it into the (17), we can obtain the complete dynamic equation of the RF-MJM, which is used in the following simulations.

3. LINEARIZATION AND LQR CONTROLLER

In this section, we first search the trim point of the RF-MJM system with one joint in steady state, and then lineariz the nonlinear model near the trim point to obtain a linear model. Finally, a LQR controller is designed.

3.1 trim point of RF-MJM system and linear of the system

A trim point (point of equilibrium) is a point at which the system is steady. Mathematically, a trim point is a point in state space of a dynamic system where the system's state derivatives equal zero. Here in this paper, the steady state is considered as

$$[\, \dot{u} \;\; \dot{v} \;\; \dot{w} \;\; \dot{p} \;\; \dot{q} \;\; \dot{r} \;\; \ddot{\theta}_1 \,]^T = 0_{7\times 1}$$

and $p = 0, q = 0, r = 0, \dot{\theta}_1 = 0$. Under these assumptions the Coriolis force and acceleration in the motion equation of RF-MJM system are zero.

Thus, the system equation will change into several nonlinear static equations and the variables to be decided are ϕ, θ, θ_1, θ_M, θ_T,a_{1s},b_{1s}. Some searching algorithm, such as trim function in Matlab, can be directly used to obtain the trim point. The result is listed out in Table2 with RF-MJM system parameters as Table1. Here, in order to evaluate the influence of the mass of the manipulator on the whole system, we compute the trim point with the different manipulator mass. With the trim point, we can get a linearized system model with the following form;

$$\Delta \dot{X} = A\Delta X + B\Delta u$$

where

$$\Delta X = [\, \Delta x \;\; \Delta y \;\; \Delta z \;\; \Delta\phi \;\; \Delta\theta \;\; \Delta\varphi \;\; \Delta\theta_1 \;\; \Delta\dot{x} \;\; \Delta\dot{y} \;\; \Delta\dot{z} \;\; \Delta\dot{\phi} \;\; \Delta\dot{\theta} \;\; \Delta\dot{\varphi} \;\; \Delta\dot{\theta}_1 \,]$$

$$A = \begin{bmatrix} 0_1 & E & 0_1 & 0_1 & 0_2 & 0_2 \\ \bar{A}_1 & \bar{A}_2 & \bar{A}_3 & \bar{A}_4 & \bar{A}_5 & \bar{A}_6 \\ 0_1 & 0_1 & 0_1 & E & 0_2 & 0_2 \\ \bar{A}_7 & \bar{A}_8 & \bar{A}_9 & \bar{A}_{10} & \bar{A}_{11} & \bar{A}_{12} \\ 0_3 & 0_3 & 0_3 & 0_3 & 0 & 1 \\ \bar{A}_{13} & \bar{A}_{14} & \bar{A}_{15} & \bar{A}_{16} & \bar{A}_{17} & \bar{A}_{18} \end{bmatrix} \tag{19}$$

$$B = [\, 0_{5\times 3} \;\; \bar{B}_1^T \;\; 0_{5\times 3} \;\; \bar{B}_2^T \;\; 0_{5\times 1} \;\; \bar{B}_3^T \,]^T \tag{20}$$

0_1 is an 3-by-3 matrix of zeros,0_2 is an 3-by-1 matrix of zeros,0_3 is an 1-by-3 matrix of zeros.

Furthermore , in order to analyze the performance of system (19), the eigenvalues of a matrix are given out in Fig.3 From it , we have the following results.

1)The whole system is static-instable since it has positive eigenvalue.

2)With the increasing of the manipulator mass, the distribution of the eigenvalues will be more diverging. The real part of eigenvalue deviates from the imaginary axis, at the same time the imaginary part of eigenvalue deviates from the real axis. Finally, in order to evaluate the coupling between the RFR and the manipulator, the coupling terms $\bar{A}_5$,$\bar{A}_{11}$,$\bar{A}_{15}$,$\bar{A}_{17}$are heavy which will be shown in section 4.

Table 1. Parameters of RF-MJM system

parameter	describe	unit
m_0=9.5	the mass of rotor flying robot(RFR)	kg
m_1=2.5	the mass of manipulator	kg
$I_{0_{xx}}$=0.1634	moment of inertia of RFR	kgm^2
$I_{0_{yy}}$=0.5782	moment of inertia of RFR	kgm^2
$I_{0_{zz}}$=0.6306	moment of inertia of RFR	kgm^2
$I_{1_{xx}}$=0.1399	moment of inertia of manipulator	kgm^2
$I_{1_{yy}}$=0.1399	moment of inertia of manipulator	kgm^2
$I_{1_{zz}}$=0.00112	moment of inertia of manipulator	kgm^2
l_0=0.3	the length from the centroid of RFR	
l_1=0.4	the length of half of the first link	m
ϕ=0.0769	roll angle	rad
θ=0.0211	pitch angle	rad
ψ=any value	yaw angle	rad
θ_1=0.0211	joint movement angle	rad

Table 2. trim points corresponding different mass of manipulator

trim point	m1=2.5	m1=2	m1=1.5	m1=1	m1=0.5
ϕ	0.0769	0.0732	0.0697	0.0662	0.0626
θ	0.0211	0.0204	0.0197	0.0190	0.0183
θ_1	0.0211	0.0205	0.0198	0.0191	0.0183
θ_M	0.0436	0.0409	0.0381	0.0354	0.0326
θ_T	-0.1282	-0.1245	-0.1207	-0.1169	-0.1130
a_{1s}	0.0211	0.0204	0.0197	0.0190	0.0183
b_{1s}	0.0195	0.0169	0.0145	0.0123	0.0103

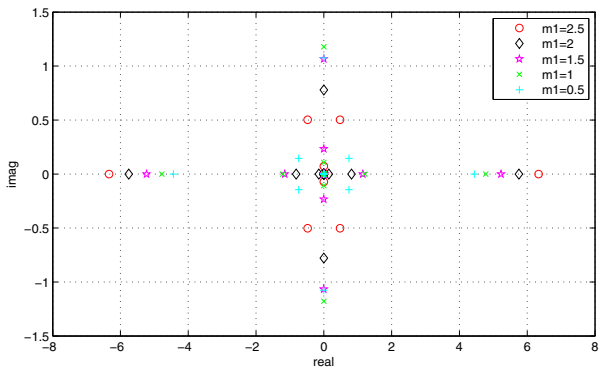

Fig. 3. eigenvalues changing of open-loop RF-MJM system with different mass of manipulator

3.2 LQR controller design

Next, we will design a full state-feedback Linear Quadratic Regulation(LQR) controller for the RFM system. In the state-feedback version of the LQR problem (Hespanha (2007)), we

assume that the whole state x can be measured and therefore it is available for control. Solution to the optimal state-feedback LQR Problem is defined more generally and consists of finding the controller variable $u(t) = -K * x(t)$ that minimizes

$$J_{LQR} := \int_0^{\infty} (x^T Q x + u^T R u) dt \tag{21}$$

where K is given by $K = R^{-1} B^T P$ and P is found by solving the continuous time algebraic Riccati equation.

$$A^T P + PA - PBR^{-1} B^T P + Q = 0$$

so we can easily get the eigenvalues of the open loop system and the closed loop system by the matrix A and $(A - B * K)$, respectively.

4. SIMULATION

In this section, two simulations are conducted to test the control performance of the RF-MJM .

A. LQR control

In this simulation, an LQR controller is designed to stablize the RF-MJM system near trim point given in the last section. Firstly, assuming the manipulator mass is m_1=2.5kg, thus the system matrix can be denoted as follows,

$$A = \begin{bmatrix} 0_1 & E & 0_1 & 0_1 & 0_2 & 0_2 \\ 0_1 & 0_1 & \bar{A}_3 & 0_1 & \bar{A}_5 & 0_2 \\ 0_1 & 0_1 & 0_1 & E & 0_2 & 0_2 \\ 0_1 & 0_1 & \bar{A}_9 & 0_1 & \bar{A}_{11} & 0_2 \\ 0_3 & 0_3 & 0_3 & 0_3 & 0 & 1 \\ 0_3 & 0_3 & \bar{A}_{15} & 0_3 & \bar{A}_{17} & 0 \end{bmatrix}$$

$$B = \begin{bmatrix} 0_4 & \bar{B}_1^T & 0_4 & \bar{B}_2^T & 0_5 & \bar{B}_3^T \end{bmatrix}$$

where

$$\bar{A}_3 = \begin{bmatrix} 0.0015 & 9.7636 & 0.9945 \\ -9.8000 & -0.0005 & 0.2102 \\ 0.0001 & 0.0005 & 0.0014 \end{bmatrix}; \quad \bar{A}_5 = \begin{bmatrix} 3.5861 \\ -0.0077 \\ 0.0310 \end{bmatrix};$$

$$\bar{A}_9 = \begin{bmatrix} -0.0087 & -0.0083 & 0.1834 \\ -0.0130 & 0.0255 & -0.8587 \\ -0.2013 & -0.2456 & -0.0635 \end{bmatrix}; \quad \bar{A}_{11} = \begin{bmatrix} -0.0547 \\ -24.4857 \\ -0.8988 \end{bmatrix};$$

$$\bar{A}_{15} = \begin{bmatrix} 0.0110 & -0.0924 & 2.6951 \end{bmatrix}; \quad \bar{A}_{17} = 40.1487;$$

$$\bar{B}_1^T = \begin{bmatrix} -0.5451 & -7.9183 & -147.7390 \\ -1.2434 & -9.3478 & 0.6158 \\ -21.7522 & 0.4534 & -0.2015 \\ -0.5829 & 7.2377 & -0.7650 \\ 0.2990 & -0.0006 & 0.0009 \end{bmatrix};$$

$$\bar{B}_2^T = \begin{bmatrix} 16.7653 & -2.5282 & 168.3611 \\ -32.8659 & 14.0449 & 125.4196 \\ 20.9082 & 178.3726 & 4.0958 \\ -121.2649 & 11.0285 & -0.2925 \\ 0.0011 & 0.6932 & -0.0534 \end{bmatrix};$$

$$\bar{B}_3^T = \begin{bmatrix} -3.9371 & -9.0113 & -99.1817 & -4.2009 & 3.4137 \end{bmatrix}$$

from these equations ,we can see that the coupling between the manipulator and helicopter $\bar{A}_5$,$\bar{A}_{11}$,$\bar{A}_{15}$,$\bar{A}_{17}$ is clear and heavy. Designing Parameters of the LQR controller are as follows,

$$Q = diag([\,1\ 1\ 1\ 1\ 1\ 1\ 10\ 10\ 10\ 10\ 10\ 10\ 10\ 10\,])$$
$$R = diag([\,1000\ 1000\ 1000\ 1000\ 1000\,])$$

then the LQR controller is

$$K = \begin{bmatrix} K_1 & K_2 & K_3 & K_4 & K_5 \end{bmatrix}$$

$$K_1 = \begin{bmatrix} 0.0097 & -0.0037 & -0.0226 \\ 0.0119 & 0.0058 & 0.0210 \\ -0.0232 & -0.0014 & 0.0013 \\ -0.0018 & 0.0308 & -0.0066 \\ 0.0149 & -0.0006 & -0.0008 \end{bmatrix}; K_5 = \begin{bmatrix} 0.6994 & 0.1310 \\ 0.5973 & 0.1125 \\ -4.2835 & -0.8102 \\ -0.3735 & -0.0691 \\ 1.1293 & 0.2157 \end{bmatrix};$$

$$K_2 = \begin{bmatrix} 0.0200 & -0.0071 & -0.0291 \\ 0.0238 & 0.0116 & 0.0287 \\ -0.0544 & -0.0019 & 0.0031 \\ -0.0042 & 0.0575 & -0.0079 \\ 0.0308 & -0.0013 & -0.0016 \end{bmatrix}$$

$$K_3 = \begin{bmatrix} 0.0502 & 0.1489 & 0.1317 \\ -0.0816 & 0.1670 & 0.1279 \\ 0.0053 & -0.4953 & -0.3462 \\ -0.3754 & -0.0384 & -0.0293 \\ 0.0104 & 0.2401 & 0.0991 \end{bmatrix}$$

$$K_4 = \begin{bmatrix} 0.0169 & 0.0637 & 0.0751 \\ -0.0226 & 0.0663 & 0.0827 \\ -0.0015 & -0.2717 & -0.0288 \\ -0.1208 & -0.0214 & -0.0058 \\ 0.0040 & 0.1085 & 0.0073 \end{bmatrix}$$

the simulation results are given out as Fig.4-Fig.7. From these figures,it can be seen that a linear LQR controller can stablize the whole system near the trim point,but here we use the joint torque of the manipulator as one of the control inputs. However, the stabilizing region of LQR is very limited, we have tested that only when the attitude of the whole system satisfied the following conditions, the LQR control can stabilize the RF-MJM system in the steady state.

$$-0.0619 \leq \theta_1 \leq 0.0611 \tag{22}$$

$$-0.6731 \leq \phi \leq 0.5469 \tag{23}$$

$$-0.1389 \leq \theta \leq 0.3911 \tag{24}$$

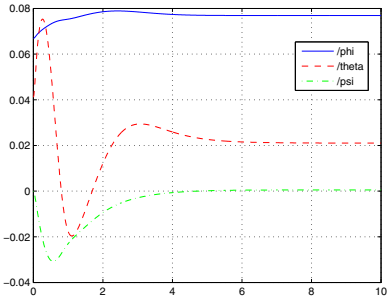

Fig. 4. roll, pitch, yaw angle changing under control of LQR controller

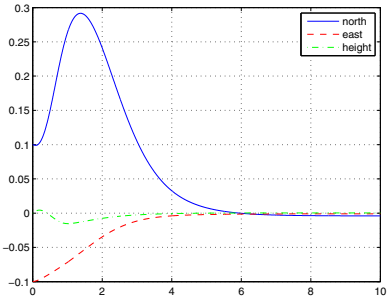

Fig. 5. position of rotor flying robot changing under control of LQR controller

B.Disturbance performance

In this simulation, a periodic sinusoid signal is added to the joint of the manipulator, as a disturbance to test the influence on the closed system. Two tests are conducted with two different disturbance: $0.01 * \sin(\pi * 0.1 * t)$ and $0.01 * \sin(\pi * 0.5 * t)$. The results are shown in Fig.8-Fig.10.From these figures, we can see that the LQR controller can attenuate some disturbances with small magnitude and frequency.

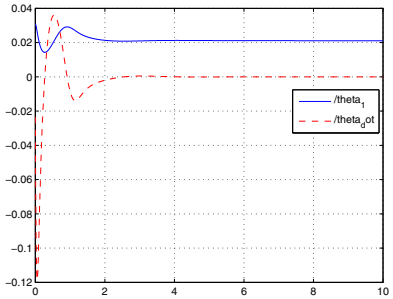

Fig. 6. angle and angle velocity of manipulator under control of LQR controller

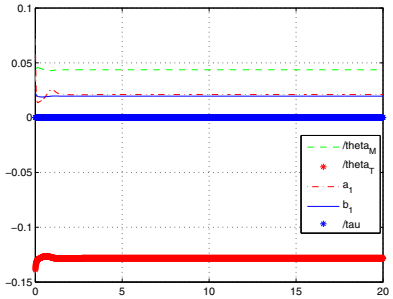

Fig. 7. control input changing under control of LQR controller

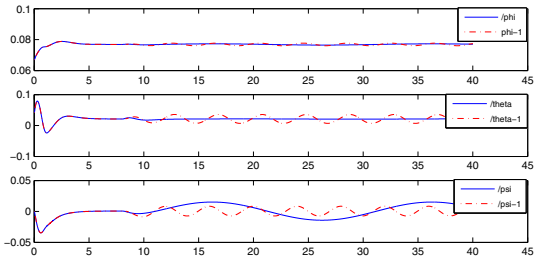

Fig. 8. roll, pitch, yaw angle changing under two kinds of control torque of the manipulator

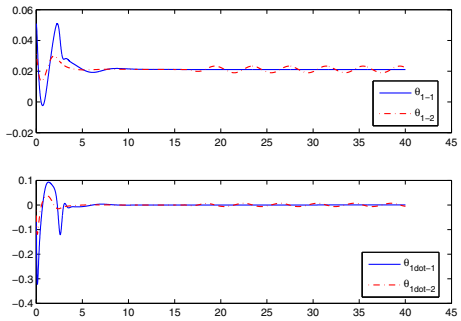

Fig. 9. angle and angle velocity of manipulator under two kinds of control torque of the manipulator

5. CONCLUSIONS

In this paper, the dynamic model of a Rotor-Flying Multi-Joint(RF-MJM)system, which is composed of a rotor-flying vehicle and a multi-joint manipulator, is constructed through using Euler-Lagrange method. By comparison to the rotor flying vehicle system, the nonlinearities and complexity increasing of the new RF-MJM can be clearly observed. Subsequently, linearizational analysis is conducted with respect to this model, the trim points with different manipulator mass are obtained to show the influence of the manipulator mass on the system's local performance, a LQR controller is designed by taking both the joint torque of the manipulator and the input of the RFR system as input. Finally, simulations are conducted and the results show that 1) a linear LQR controller can stablize the system near hovering state, but it's stabilization region is not large enough; 2)the linear LQR controller is sensitive to the external disturbance. In future works, nonlinear control method will be used to overcome the disadvantages of the linear controller.

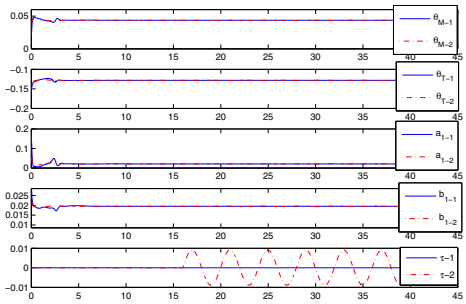

Fig. 10. control input changing under two kinds of control torque of the manipulator

REFERENCES

Bernard, M. and Kondak, K. (2009). Generic slung load transportation system using small size helicopters. In *Robotics and Automation, 2009. ICRA'09. IEEE International Conference on*, 3258–3264. IEEE.

Birk, A., Wiggerich, B., Bülow, H., Pfingsthorn, M., and Schwertfeger, S. (2011). Safety, security, and rescue missions with an unmanned aerial vehicle (uav). *Journal of Intelligent & Robotic Systems*, 57–76.

Bolkcom, C. (2004). Homeland security: Unmanned aerial vehicles and border surveillance.

Bramwell, A.R., Balmford, D., and Done, G. (2001). *Bramwell's helicopter dynamics*. Butterworth-Heinemann.

Cai, G., Chen, B.M., and Lee, T.H. (2010). An overview on development of miniature unmanned rotorcraft systems. *Frontiers of Electrical and Electronic Engineering in China*, 5(1), 1–14.

He, Y. and Han, J. (2010). Acceleration-feedback-enhanced robust control of an unmanned helicopter. *Journal of guidance, control, and dynamics*, 33(4), 1236–1250.

Hespanha, J. (2007). Undergraduate lecture notes on lqg/lqr controller design. *Apuntes para Licenciatura. UCBS (University of California, Santa Barbara)*, 1–37.

Mellinger, D., Shomin, M., Michael, N., and Kumar, V. (2013). Cooperative grasping and transport using multiple quadrotors. In *Distributed autonomous robotic systems*, 545–558. Springer.

Pounds, P.E., Bersak, D.R., and Dollar, A.M. (2011). Grasping from the air: Hovering capture and load stability. In *Robotics and Automation (ICRA), 2011 IEEE International Conference on*, 2491–2498. IEEE.

Puri, A. (2005). A survey of unmanned aerial vehicles (uav) for traffic surveillance. *Department of computer science and engineering, University of South Florida*.

Shim, D.H. (2000). *Hierarchical control system synthesis for rotorcraft-based unmanned aerial vehicles*. Ph.D. thesis, Berkeley.

Valavanis, K.P. (2007). *Advances in unmanned aerial vehicles: state of the art and the road to autonomy*, volume 33. Springer.

Yoshida, K. and Umetani, Y. (1993). Control of space manipulators with generalized jacobian matrix. *Space robotics: Dynamics and control*, 165–204.